

Zn impurity induced moments and tunneling conductance asymmetry in cuprate superconductors

Jaesung Yoon, Tae-Hyoung Gimm, Hyun C. Lee, and Han-Yong Choi

*Department of Physics, BK21 Physics Research Division,
and Institute for Basic Science Research,
Sung Kyun Kwan University, Suwon 440-746, Korea.*

(Dated: November 18, 2018)

Abstract

The effects of a non-magnetic Zn impurity substituting an in-plane Cu are studied by solving the Bogoliubov-de Gennes equation self-consistently which is derived from the t - t' - J - U Hamiltonian with all the allowed order parameters included. The Zn impurity, modeled in terms of a potential scatterer in unitary limit, induces local staggered magnetic moments around itself, and the calculated NMR shifts from the induced moments are in agreement with the experimental Cu NMR spectra. We also note that the experimentally observed negative slope of the tunneling conductance can result from the next-nearest hopping t' .

After more than a decade of intensive research on the high T_c superconductors, we are still far from a coherent understanding of the underlying physics [1]. One informative route of study is provided by the impurities like Zn and Ni, which substitute for Cu sites in the CuO_2 planes where the superconductivity (SC) is believed to emerge from. Therefore, the impurity induced information about the SC and magnetism and their correlation can provide a clue to the underlying physics of the high T_c SC in that a common feature of the cuprates is the proximity of the antiferromagnetism and SC. The high resolution atomic scale probes on the impurity substituted cuprates provide important information in this regard. For instance, Pan *et al.* reported the scanning tunneling microscopy (STM) study on a Zn substituted $\text{Bi}_2\text{Sr}_2\text{CaCu}_2\text{O}_{8+\delta}$, that is, the tunneling conductance as a function of the atomic position and bias voltage, $G(\vec{r}, V)$ [2]. They observed among others that (a) at $\vec{r} = \text{Zn}$ site, there is a strong peak in $G(\vec{r}, V)$ as a function of V near zero bias voltage ($V \approx -1.5$ meV), (b) at $V = -1.5$ meV, the real space distribution of the intensity $G(\vec{r}, V)$ shows local maxima at next-nearest Cu sites from the Zn, and (c) the spatially averaged conductance $\int d\vec{r}G(\vec{r}, V)$ has a negative slope as a function of V . Also, several groups reported NMR experiments on Zn [3, 4], Li [5], or Ni [6] substituted $\text{YB}_2\text{Cu}_3\text{O}_{7-x}$. It was found that (d) local staggered moments were induced and SC was destroyed around the impurity site, and away from there the induced moments become vanishing and the pairing amplitudes heal back to the bulk value.

Interpretation of these observations at present is controversial. For the observations (a) and (b), some groups proposed the blocking or interference effects [7, 8], but other groups introduced the Kondo effect due to the impurity induced magnetic moments [9]. For the observation (c), Rantner and Wen suggested from a $SU(2)$ slave boson mean-field calculation that the asymmetric tunneling background may be due to the strong onsite repulsion [10]. Although there are quite a few theoretical works on the magnetic or non-magnetic impurity effects on superconductivity [11, 12, 13, 14], no theoretical calculation of the induced magnetic moments due to a non-magnetic impurity in a SC state has been reported yet. We report such a calculation in this paper. We study the t - t' - J - U Hamiltonian with the Zn impurity modeled as a potential scatterer near the unitary limit to understand the observations (c) and (d) listed above.

In order to address the observations (c) and (d), we consider the t - t' - J - U model given as

follows:

$$\begin{aligned}
H = & \sum_{\langle\langle i,j \rangle\rangle\sigma} [(-t_{ij} - \mu\delta_{ij})c_{i\sigma}^+c_{j\sigma} + h.c.] + J \sum_{\langle i,j \rangle} \left(\widehat{S}_i \cdot \widehat{S}_j - \frac{\widehat{n}_i\widehat{n}_j}{4} \right) \\
& + U \sum_i \widehat{n}_{i\uparrow}\widehat{n}_{i\downarrow} + V_{imp} \sum_{\sigma} c_{i_0\sigma}^+c_{i_0\sigma},
\end{aligned} \tag{1}$$

where $\widehat{n}_{i\sigma} = c_{i\sigma}^+c_{i\sigma}$, $\widehat{n}_i = \sum_{\sigma} \widehat{n}_{i\sigma}$, \widehat{S}_i the spin-1/2 operator, μ the chemical potential, U the onsite Hubbard repulsion, V_{imp} the impurity potential at the Zn impurity site i_0 , and J is the nearest neighbor exchange integral. The $\langle\rangle$ and $\langle\langle\rangle\rangle$ stand for the summations up to, respectively, the nearest and next-nearest neighbors, and t_{ij} is equal to t for the nearest and to t' for the next-nearest neighbors. The normal state band structure is then given by

$$\epsilon_k = -2t[\cos(k_x a) + \cos(k_y a)] - 4t' \cos(k_x a) \cos(k_y a). \tag{2}$$

Note that we included both U and J in the Hamiltonian. This was motivated by the recent work by Daul *et al.* who suggested that the t - U - J model be more appropriate than the t - J or Hubbard models to describe the real cuprate system by allowing the charge fluctuations with the finite Hubbard U [15].

The t - t' - J - U model of Eq. (1) was treated with the Hartree-Fock-Bogoliubov (HFB) approximation to yield the Bogoliubov-de Gennes (BdG) equation in the real space. It was then solved via iterations with all the allowed order parameters determined self-consistently, that is, the d -wave pairing, bond, charge, and spin order parameters. We found that (1) local antiferromagnetic moments are induced due to a non-magnetic impurity, (2) the tunneling conductance shows a negative slope as a function of bias voltage V due to the next-nearest neighbor hopping t' , and (3) the local density of states (LDOS) at the 4 nearest neighbors shows a peak near zero energy. The calculated NMR spectra from the distribution of the induced magnetic moments is found to be in agreement with the experimentally observed ^{63}Cu NMR spectra [4]. There is some controversy in understanding the experimental observations (a) and (b) with the result (3) as mentioned before. Here, we will report the results (1) and (2) in more detail to understand the observations (c) and (d).

The BdG equation derived from the Hamiltonian of Eq. (1) within the HFB approximation can be written as

$$\sum_j \begin{pmatrix} H_{ij\downarrow} & \Delta_{ij}\delta_{i+\tau,j} \\ \Delta_{ij}^*\delta_{i+\tau,j} & -H_{ij\uparrow} \end{pmatrix} \begin{pmatrix} u_{j,n} \\ v_{j,n} \end{pmatrix} = E_n \begin{pmatrix} u_{i,n} \\ v_{i,n} \end{pmatrix}, \tag{3}$$

where

$$\begin{aligned}
H_{ij\sigma} = & -(t + J\chi_{ij,-\sigma}^*)\delta_{i+\tau,j} + (Un_{i,-\sigma} - \mu)\delta_{ij} \\
& - Jn_{i,-\sigma}\delta_{i+\tau,j} - t'\delta_{i+\tau',j} + V_{imp}\delta_{i,i_0},
\end{aligned} \tag{4}$$

and the subscripts τ and τ' are, respectively, the nearest and next-nearest neighbors. The order parameters, d -wave pairing Δ_{ij} , bond-order $\chi_{ij\sigma}$, spin up and down charge densities $n_{i\sigma}$, were determined from the following self-consistency conditions:

$$\begin{aligned}
\Delta_{ij} &= J(\langle c_{i\uparrow}c_{j\downarrow} \rangle + \langle c_{j\uparrow}c_{i\downarrow} \rangle) = J \sum_n [u_{j,n}v_{i,n}f(-E_n) + u_{i,n}v_{j,n}f(-E_n)], \\
\chi_{ij\uparrow} &= \langle c_{i\uparrow}^+c_{j\uparrow} \rangle = \sum_n u_{i,n}^*u_{j,n}f(E_n), \\
\chi_{ij\downarrow} &= \langle c_{i\downarrow}^+c_{j\downarrow} \rangle = \sum_n v_{i,n}^*v_{j,n}f(-E_n), \\
n_{i\uparrow} &= \langle \hat{n}_{i\uparrow} \rangle = \sum_n u_{i,n}^*u_{i,n}f(E_n), \\
n_{i\downarrow} &= \langle \hat{n}_{i\downarrow} \rangle = \sum_n v_{i,n}^*v_{i,n}f(-E_n),
\end{aligned} \tag{5}$$

where $\langle \dots \rangle$ represents the thermodynamic average and $f(\omega) = 1/[1 + \exp(\beta\omega)]$ is the Fermi distribution function. Charge and spin densities are then given by $n_i = n_{i\uparrow} + n_{i\downarrow}$ and $S_z(\vec{i}) = \frac{1}{2}(n_{i\uparrow} - n_{i\downarrow})$, respectively. Eq. (3) with the self-consistency conditions of Eq. (5) was solved via iterations with a unit cell of 20×20 , or 30×30 sites using a periodic boundary condition with 5×5 wave-vector points in the first quadrant of the Brillouin zone. The LDOS which is proportional to the tunneling conductance, and local magnetic moments of the i -th site can be obtained from

$$\begin{aligned}
D(\vec{i}, \omega) &= \sum_{n,k} [|u_{i,nk}|^2 \delta(\omega - E_{nk}) + |v_{i,nk}|^2 \delta(\omega + E_{nk})], \\
S_z(\vec{i}) &= \frac{1}{2} \sum_{n,k} [|u_{i,nk}|^2 f(E_{nk}) - |v_{i,nk}|^2 f(-E_{nk})].
\end{aligned} \tag{6}$$

A few remarks about the Hamiltonian are in order. The bond-order, although not essential, was included because (a) it is an allowed order parameter in the t - t' - J - U model unlike in a model with the onsite repulsion U and next-nearest-neighbor attraction V (t - t' - U - V , or minimal model), and (b) it was found important for stabilizing the bond-centered stripes where the more sophisticated methods like the density matrix renormalization group predict so and the half-filled metallic stripes as observed experimentally [17]. We wished to use a model of more general validity applicable for both the impurity and stripe problems. This

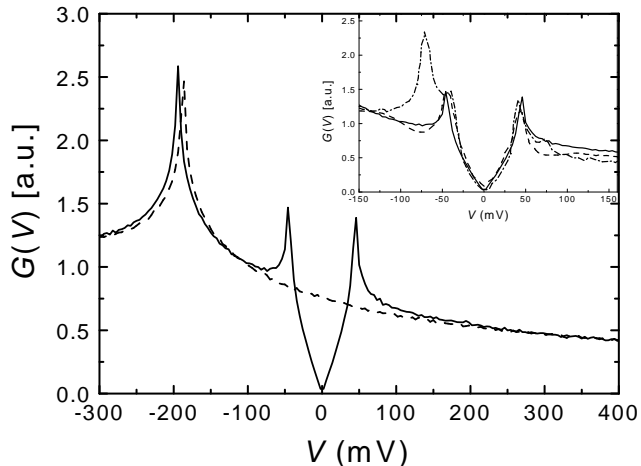


FIG. 1: The tunneling conductances in normal (dashed) and SC (solid curve) states. In the inset, TDOS in SC state in the main figure is shown in more detail around the gap feature and is compared with the Pan *et al.* experiment (dashed curve) and Rantner and Wen calculation (dot-dashed).

is the main reason we employed the t - t' - J - U model in the present study. On the other hand, the physics discussed here may also be described in terms of the minimal model because the bond-order is not essential for the moment induction.

Let us first consider the asymmetric tunneling background of the observation (c). We take the parameters $t = 0.4$ eV, $t' = -0.45 t$, $U = 3 t$, and $J = 0.75 t$, which are appropriate for $\text{Bi}_2\text{Sr}_2\text{CaCu}_2\text{O}_{8+\delta}$. Rather a large value of J was necessary to fit the pairing amplitude $\Delta = 48$ meV observed in the Pan *et al.* STM experiment. To illustrate the point in a simple way, we put $S_z = 0$. Fig. 1 shows the tunneling density of states (TDOS) in normal (dashed) and SC state (solid line) at the 16 % doping concentration. The two-dimensional tight-binding band given by Eq. (2) has a van Hove singularity (vHS) due to a logarithmic divergence. The vHS, or a peak in DOS occurs at the band center for $t' = 0$. But, for $t' < 0$ the peak in the DOS moves to a lower energy relative to the Fermi level and, consequently, the DOS has a negative slope around the Fermi level ($\omega = 0$) as a function of the bias voltage as shown in the Fig. 1. Small offset of the vHS peaks between the normal and SC states are due to the pairing and the difference in the bond orders, and the V-shape around $\omega = 0$ of the solid curve is due to the d -wave pairing. This is shown in more detail

around the gap feature in the inset. The solid, dashed, and dot-dashed curves represent, respectively, the present calculation, Pan *et al.* data, and Rantner and Wen calculation. The agreement of the present calculation with the Pan *et al.* data is quite satisfactory without fine adjustments. It seems natural, therefore, to understand the observed negative slope of the tunneling background [2, 16] in terms of the particle-hole symmetry breaking around the band center because of the next-nearest hopping integral t' . Rantner and Wen, on the other hand, argued that the asymmetric tunneling background can be explained in terms of $SU(2)$ slave-boson approach [10]. But the present explanation is more straightforward, and fits the experimental observation much better than their calculation. Interactions may bring in some corrections in the tunneling conductance but the background slope will be mainly set by the particle-hole symmetry breaking due to the t' . We therefore believe that the asymmetric tunneling background is most probably due to the next-nearest hopping integral t' .

Now we turn to the main result of the present work, that is, the magnetic moment formation due to a Zn impurity substituting an in-plane Cu site of the cuprate superconductors. We took $J = t$, $T = 0.0005 t$, and all other parameter values the same as in Fig. 1. A slightly larger value of J was taken to show the doping induced features more clearly. This set of parameters yields the pairing $\Delta = 0.312 t$, magnetic moment $S_z(\vec{i}) = 0$, and bond order $\chi_\sigma = 0.18 t$. The doping level was set such that (i) the self-consistently determined S_z vanishes without the impurity and (ii) the chemical potential is higher than the vHS energy. The requirement of (i) ensures that the moments do not exist *without* the Zn impurity, and (ii) ensures that the tunneling conductance background has a negative slope around the Fermi level. In the present HFB mean-field calculation, these two requirements are met around 40 – 55 % doping for $t' = -0.45 t$ depending on U and J . This extremely high doping concentration, an artifact of the mean-field calculation which could be cured by going beyond the mean-field theory, was caused by the requirements of negative tunneling conductance slope and the large (realistic) t' . These constraints were not properly considered previously. Although the present calculations can also be done around 15 % doping without the constraints, they were done at a high doping level with the experimental constraints satisfied. The reason is that the induced moments are not affected much by the largeness of the doping level since they are mainly determined by the competition of the electron kinetic energy and the effective exchange integral. This has been checked by direct numerical calcu-

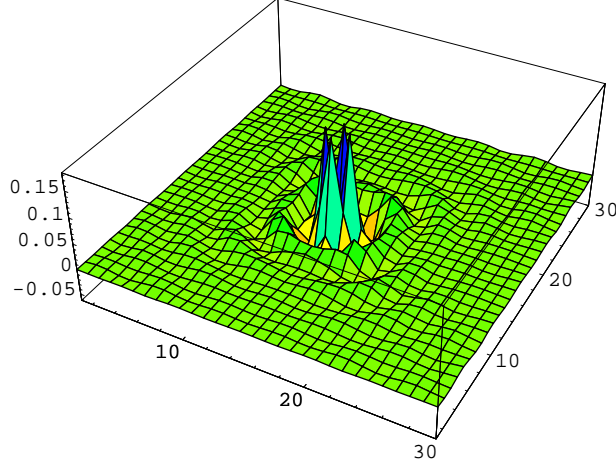


FIG. 2: The staggered magnetic moments $\tilde{S}_z(\vec{i})$ induced around an non-magnetic impurity at $T = 0.0005 t$, for $J = t$, $t' = -0.45 t$, and $U = 3 t$. Note that the induced moments reside mainly on the 4 nearest neighbors and exhibit a Friedel-like oscillation.

lations without the requirements, and is further strengthened by the satisfactory agreement of the computed NMR spectra from the induced moments with experiments as is discussed in Fig. 3. On the other hand, the resonant energy and peak strength depend on the parameters of the model like the t' , V_{imp} , and doping concentration somewhat sensitively as noted previously [18], and some care must be taken before comparing different calculations.

We took $V_{imp} = -100 t$ to model a Zn impurity placed at $\vec{i} = (15,15)$ in a 30×30 unit cell. Fig. 2 shows the staggered magnetic moments $\tilde{S}_z(\vec{i}) = (-1)^{(i_x+i_y)} S_z(\vec{i})$ induced by the Zn. Antiferromagnetic moments develop with the peaks at the four nearest sites around the impurity site. The total spin $\sum_i S_z(\vec{i}) = \frac{1}{2}\hbar$. The magnetic moment vanishes at the impurity site, and the Zn remains non-magnetic. The Friedel-like concentric oscillation with a period of 3 – 4 lattice constants can clearly be seen. The oscillation exhibits an angular anisotropy as expected; along the anti-nodal direction it gets more suppressed because of the pairing gap and along the nodal direction it shows more pronounced oscillation. The d -wave pairing gap, $\tilde{\Delta}_d(\vec{i}) = [\Delta_{\vec{i},\vec{i}+x} + \Delta_{\vec{i},\vec{i}-x} - \Delta_{\vec{i},\vec{i}+y} - \Delta_{\vec{i},\vec{i}-y}]/2$, remains $0.312 t$ for most of unit cell, but on the impurity site $\tilde{\Delta}_d(\vec{i})$ vanishes. The superconductivity is severely destroyed by the non-magnetic impurity within about 2 lattice constants around the impurity site.

From the Zn impurity-induced $S_z(\vec{i})$ shown in Fig. 2, we have also calculated the broadened NMR spectra which may be compared with the experimental ^{63}Cu NMR spectra.

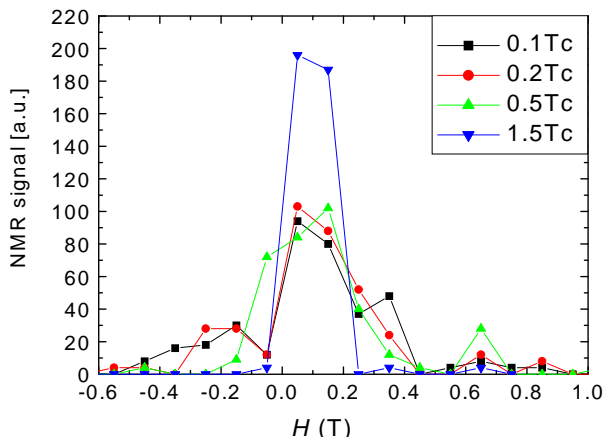


FIG. 3: The Cu NMR spectra calculated from the distribution of the induced magnetic moments due to a Zn impurity as shown in Fig. 2.

The NMR spectra is just a histogram of the frequency shifts given by $h_i = A_\alpha^{onsite} S_z(\vec{i}) + B \sum_\tau S_z(\vec{i} + \vec{\tau})$, where $A_\alpha^{onsite} = -13.8 T/\mu_B$ and $B = 3.45 T/\mu_B$ for the magnetic field $\vec{H} \parallel c$ -axis [4]. The T -dependence of the induced moments were calculated for several different T with a 20×20 unit cell. The distribution of the induced moments in 20×20 unit cell is almost the same with the 30×30 one because the magnetic correlation length is shorter than the unit cell size. The results at $T = 0.1 T_c$, $0.2 T_c$, $0.5 T_c$, and $1.5 T_c$ are shown in Fig. 3. The width of the NMR spectra gets narrower as T is increased because the induced moments are decreased. Compared with the NMR spectra [Fig. 1(a) in Ref. [4]], the results are quite satisfactory, which gives a reliability to the present calculation of the induced magnetic moments.

There are two factors that contribute to the induction of the magnetic moments by a non-magnetic impurity: the localization of an electron and destruction of superconductivity around the impurity site due to the deep impurity potential of the Zn. The magnetic moment in a normal state is determined by the competition between the effective exchange integral of $2J + U$ and the electron hopping motion of t . When an electron is localized by the impurity potential, the electron hopping gets suppressed, which favors the appearance of magnetic moments around the impurity site, as was studied by Odashima and Matsumoto in a normal state [19]. In a SC state, the appearance of magnetic moments can also be suppressed by the onset of superconductivity. Therefore, when the superconductivity is destroyed by an

impurity, magnetic moments can appear around the impurity site. Both of above two factors contribute to the appearance of the magnetic moments induced by the Zn impurity in a SC state. Similar ideas were suggested by various groups in the context of spin gaped systems [20, 21]. The idea was that the freed spins created by an impurity abide by the impurity site because of the confinement provided by antiferromagnetic correlations and show up around the impurity. The present theory can readily be applied to the magnetic impurity effects such as the recent STM experiment on Ni substituted $\text{Bi}_2\text{Sr}_2\text{CaCu}_2\text{O}_{8+\delta}$ [22]. We are currently carrying out such calculations and will report the results elsewhere.

To summarize, we considered the t - t' - J - U Hamiltonian to study the non-magnetic Zn impurity effects in d -wave superconductivity. The Bogoliubov-de Gennes equation in the real space was derived from the Hamiltonian using the Hartree-Fock-Bogoliubov approximation, and was solved self-consistently with the d -wave pairing, bond, charge, and spin order parameters included. It was demonstrated that a non-magnetic impurity induces the antiferromagnetic moments around itself in a d -wave superconductive state. The calculated NMR spectra due to the induced moments are found to be in good agreement with the experiments. It was also proposed that the negative slope of the tunneling conductance may most probably come from the next-nearest hopping integral t' .

We would like to thank Sasha Balatsky for helpful discussions. This work was supported by the Korea Science & Engineering Foundation (KOSEF) through the grant No. 1999-2-11400-005-5, by the Korea Research Foundation (KRF) through the grant No. KRF-2000-DP0139, and by the Ministry of Education through the Brain Korea 21 SNU-SKKU Physics Program.

-
- [1] D. M. Ginsberg, *Physical Properties of High Temperature Superconductors* Vol. I - V (World Scientific).
 - [2] S. H. Pan *et al.*, Nature (London) **403**, 746 (2000).
 - [3] H. Alloul *et al.*, cond-mat/9905424.
 - [4] M. H. Julien *et al.*, Phys. Rev. Lett. **84**, 3422 (2000).
 - [5] J. Bobroff *et al.*, Phys. Rev. Lett. **86**, 4116 (2001).
 - [6] G. V. M. Williams, J. L. Tallon, and R. Dupree, Phys. Rev. B **61**, 4319 (2000).

- [7] I. Martin, A. V. Balatsky, and J. Zaanen, cond-mat/0012446.
- [8] J. X. Zhu, C. S. Ting, and C. R. Hu, Phys. Rev. B **62**, 6027 (2000).
- [9] A. Polkovnikov, S. Sachdev, and M. Vojta, Phys. Rev. Lett. **86**, 296 (2001).
- [10] W. Rantner and X. G. Wen, Phys. Rev. Lett. **85**, 3692 (2000).
- [11] A. V. Balatsky, M. I. Salkola, and A. Rosengren, Phys. Rev. B **51**, 15547 (1995).
- [12] M. I. Salkola, A. V. Balatsky, and D. J. Scalapino, Phys. Rev. Lett. **77**, 1841 (1996).
- [13] M. I. Salkola, A. V. Balatsky, and J. R. Schrieffer, Phys. Rev. B **55**, 12648 (1997).
- [14] C. H. Choi, Phys. Rev. B **63**, 064507 (2001).
- [15] S. Daul, D. J. Scalapino, and S. R. White, Phys. Rev. Lett. **84**, 4188 (2000).
- [16] A. Yazdani *et al.* Phys. Rev. Lett. **83**, 176 (1999).
- [17] T. H. Gimm *et al.*, to be published in Physica C.
- [18] I. Martin and A. V. Balatsky, cond-mat/0003142.
- [19] S. Odashima and H. Matsumoto, Phys. Rev. B **56**, 126 (1997).
- [20] R. Kilian, S. Krivenko, G. Khaliullin, and P. Fulde, Phys. Rev. B **59**, 14432 (1999).
- [21] S. Sachdev and M. Vojta, cond-mat/0009202.
- [22] E. W. Hudson *et al.*, Nature (London) **411**, 920 (2001); M. E. Flatte, *ibid.*, 901 (2001).